Kárahnjúkar Dam spillway, Iceland: Swiss contribution to reduce dynamic plunge pool pressures generated by a high-velocity jet

Thomas Berchtold, Michael Pfister

Abstract: *Spillways often include a flip bucket as terminal energy dissipator, combined with a plunge pool. For large jet fall heights, the residual energy may provoke scour at the river bed. Additional measures are then required, such as chute widening, increase of the plunge pool depth, or insertion of baffles at the chute end. The effect of these measures was investigated in hydraulic modelling. The dynamic plunge pool bottom pressures in the jet footprint area were systematically recorded. Both the time-averaged and the fluctuating dynamic pressure heads are considered as references for the jet scour potential, beside the related pressure coefficients. The investigated measures were proven to be effective in terms of reduced pressures, especially in combination. This research relates to the Kárahnjúkar spillway model investigation, in which the principal working conditions as canyon topography, jet fall head and discharge spectrum were determined. The relevant parameters of the herein presented measures were systematically varied in a wider range, independent of the project.*

1. Introduction

Most reservoirs include a spillway to convey floods, thereby avoiding dam overtopping. They typically spill extreme discharges with a large head, resulting in high-velocity flows. Chute flows have a considerable energy at the spillway end, which has to be adequately dissipated upstream of the receiving waters (Lopardo 1988, Fiorotto and Rinaldo 1992, Puertas and Dolz 2005, Khatsuria 2005). Otherwise, large scour emerges which may destabilize the dam foundation or erode adjacent valley flanks, and generate sediment deposits further downstream. High-head spillways therefore often include a flip bucket with a plunge pool (Vischer and Hager 1998).

Despite of jet disintegration and diffusion within the plunge pool (Ervine et al. 1997), jets may provoke unacceptable scour for a large fall height combined with a limited plunge pool depth (Bollaert and Schleiss 2003a, b). Additional measures are then necessary to enhance the jet disintegration process, thereby minimizing its energy entrainment into the plunge pool (Ervine and Falvey 1987, Annandale 2005, Bollaert and Schleiss 2005, Pagliara et al. 2006, Li and Liu 2010). These additional measures normally include elements to increase jet turbulence, such as baffles mounted at the spillway end or spillway width increase to generate thinner jets. Jet disintegration, spreading and aeration are thereby enhanced (Canepa and Hager 2003, Schmocker et al. 2008, Pfister and Hager 2009), reducing specific energy density at the jet footprint on the plunge pool bottom. Ervine et al. (1997) mention that jet diffusion in the plunge pool is furthermore relevant for limited pressure fluctuations on the pool bottom, and that air entrained by the jet reduces bottom pressure amplitudes. The dynamic pressure characteristics at the pool bottom in shallow and deep pools usally follow a Gaussian distribution, as shown by Manso et al. (2007).

This research presents measures affecting a free jet issued from a spillway to reduce plunge pool pressures. The results were derived from a physical model investigation conducted at the Laboratory of Hydraulics, Hydrology and Glaciology (VAW), ETH Zurich. This project was initiated by the related Kárahnjúkar spillway investigation (VAW 2006, Pfister et al. 2008), in terms of topography, net fall head and discharge spectrum. However, the relevant parameters of this work were systematically varied in a wide range, independent of the original project. The national power company of Iceland, Landsvirkjun, commissioned the 690 MW Kárahnjúkar Hydroelectric Project in Eastern Iceland in 2008 for the electric supply of an aluminum smelter. It includes three dams storing the Hálslón reservoir with a water volume of $2.1 \cdot 10^9$ m^3. An unregulated spillway is located at the left embankment of the 198 m high main dam *(Fig. 1a)*, consisting of a side channel, a transition bend and a 419 m long chute. It was designed for a discharge of 1350 m^3/s, and evacuates a PMF of 2250 m^3/s (Tómasson et al. 2006). At the chute end, the water falls as a free jet into a narrow canyon with almost 100 m high vertical rock flanks *(Fig. 1b)*. These are unstable due to cracks and soft rock, such that measures to reduce the scour potential of the jet were sought. A tailwater dike resistant to overflow erosion impounds a plunge pool on the riverbed.

2. Characteristic plunge pool pressures

The following pressure heads in [m] water column are considered:

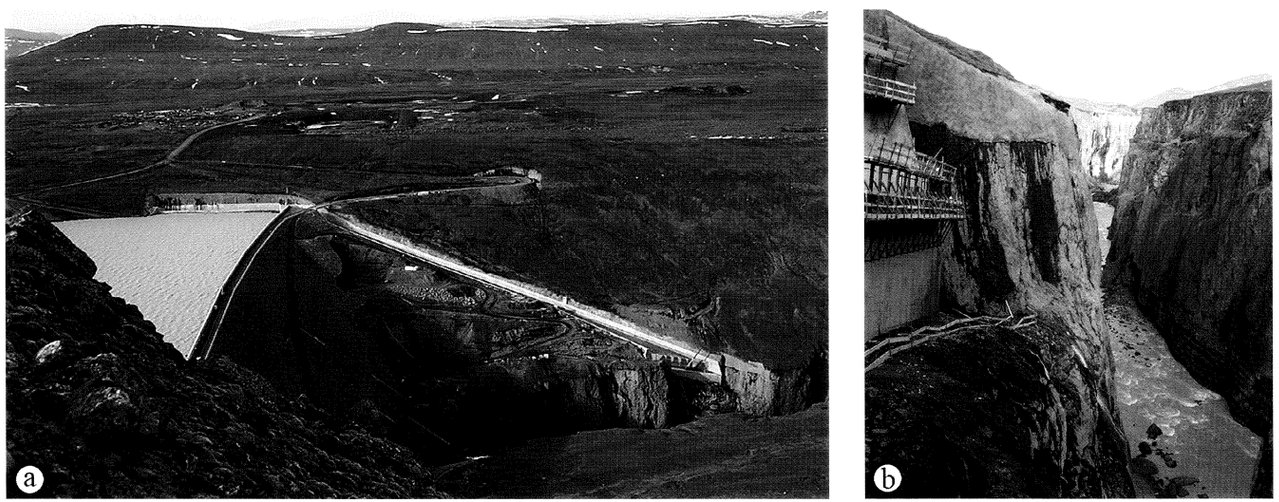

Figure 1. (a) Overview of Kárahnjúkar Dam and spillway above canyon (courtesy Landsvirkjun), and (b) canyon in flow direction with chute end at left; tailwater dike was not yet constructed.

- Effective (subscript *e*) measured, instantaneous (subscript*i*) transmitter pressure head P_{ei}.
- Hydrostatic pressure head *Y* defined as vertical elevation difference between the transmitter level and tail water dike crest. This simplification overlooks the high degree of turbulence and air entrainment within the plunge pool which inhibits the recording of a precise hydrostatic pressure head.
- Dynamic (subscript *d*) instantaneous pressure head $P_{di} = P_{ei} - Y$.
- Time-averaged (subscript *a*) dynamic pressure head P_{da} and respective average dynamic pressure coefficient C_{da} as

$$P_{da} = \frac{\sum P_{di}}{N} \tag{1}$$

$$C_{da} = P_{da}\left(\frac{v_j^2}{2g}\right)^{-1} \tag{2}$$

with *N* as number of pressure head records, and *g* as acceleration of gravity. The jet impact velocity v_j on the plunge pool water surface was derived from the hydraulic model using high-speed particle tracking and from energy considerations.

- Fluctuating dynamic pressure head P'_d and respective fluctuating dynamic pressure coefficient C'_d as

$$P'_d = \sqrt{\frac{\sum (P_{da} - P_{di})^2}{N}} \tag{3}$$

$$C'_d = P'_d\left(\frac{v_j^2}{2g}\right)^{-1} \tag{4}$$

3. Hydraulic model

The physical model was built for the Kárahnjúkar investigation with a scale factor of 45 and operated using Froude similitude (*Fig. 2a*, VAW 2006). It reproduced a sector of the Hálslón reservoir, the entire spillway, a section of the canyon and the complete plunge pool including the tailwater dike. The canyon bed was rigid, i.e. no scour occurred in the model thereby allowing for dynamic pressure measurements. The vertical extension of the Kárahnjúkar plunge pool depth is limited because: (1) plunge pool bottom elevation is restricted to avoid extensive excavation works and instability of the adjacent rock flanks, and (2) high water levels are excluded to avoid a submerged bottom outlet. The plunge pool width is 70 to 90 m restricted by the canyon dimensions (*Figs. 1* and *2*), and its length is some 400 m. The main dam toe is located 250 m upstream and the tailwater dike 150 m downstream of the jet impact. Given the narrow canyon and high discharges, a distinctive longitudinal flow component is established in the plunge pool toward the tailwater dike.

The take-off lip at the chute end is oblique relative to the flow direction, following the canyon edge. Furthermore, no flip bucket is installed, such that the chute end has the same slope of 20% as the chute. Beside constructional advantages, this design rotates the jet foot-print and adjusts it to the plunge pool shape (Pfister et al. 2008).

The discharge was determined by Inductive Discharge Measurement to ±3% accuracy. The pressure head P_{ei} was recorded in the model using transmitters, typically over 120 s. The sampling rate during dynamic acquisitions was 200 Hz and the transmitters were calibrated before each test. A movable plate with eight transmitters was fixed on the river bed to detect jet-generated pressures and their fluctuations. The entire jet footprint was thereby covered with a prototype grid spacing of 2.25 m.

The width *b* of the chute end perpendicular to the flow direction was varied between 17.0 and 30.6 m, the hydrostatic plunge pool pressure head *Y* between 5.2 and 15.2 m, the discharge *Q* between 400 and 800 m³/s, and the jet impact

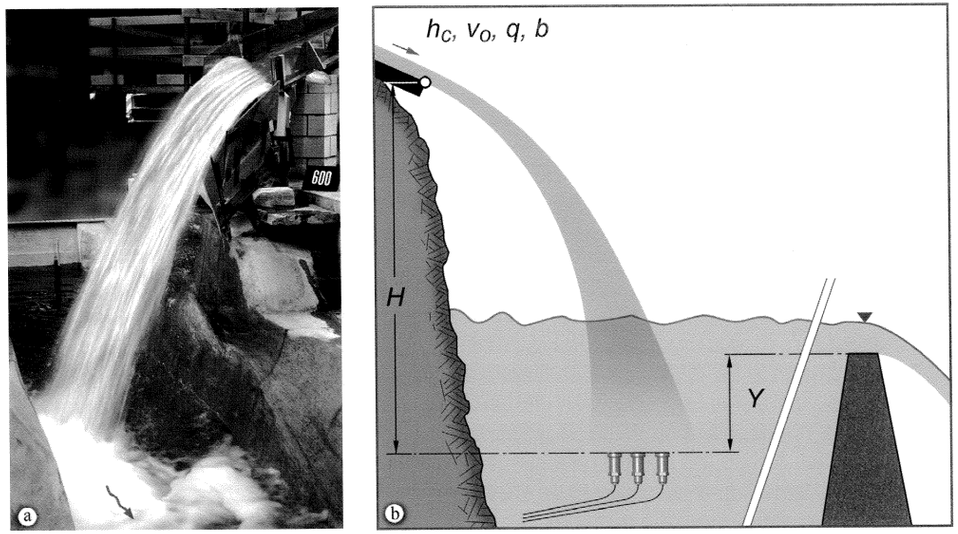

Figure 2. (a) Lower part of model spillway with canyon and plunge pool, Q = 600 m³/s, b = 30.6 m and Y = 5.2 m, and (b) definition plot.

Test Nr.		1	2	3	4	5	6	7	8	9	10	11	12
Q	[m³/s]	400	600	800	400	600	800	400	600	800	400	600	800
b	[m]	17.0	17.0	17.0	17.0	17.0	17.0	17.0	17.0	17.0	23.8	23.8	23.8
Y	[m]	5.2	5.2	5.2	10.2	10.2	10.2	15.2	15.2	15.2	5.2	5.2	5.2
P_{daM}	[m]	15.3	19.5	21.3	7.4	9.2	13.5	2.6	5.1	10.5	12.8	15.7	18.8
Test Nr.		13	14	15	16	17	18	19	20	21	22	23	24
Q	[m³/s]	400	600	800	400	600	800	400	600	800	400	600	800
b	[m]	23.8	23.8	23.8	23.8	23.8	23.8	30.6	30.6	30.6	30.6	30.6	30.6
Y	[m]	10.2	10.2	10.5	15.2	15.2	15.2	5.2	5.2	5.2	10.2	10.2	10.2
P_{daM}	[m]	3.8	7.5	8.3	2.4	3.2	4.5	8.1	11.9	13.3	2.6	5.2	7.6
Test Nr.		25	26	27		*28*	*29*	*30*					
Q	[m³/s]	400	600	800		*600*	*950*	*950*					
b	[m]	30.6	30.6	30.6		*30.6*	*30.6*	*30.6*					
Y	[m]	15.2	15.2	15.2		*6.5*	*6.5*	*11.5*					
P_{daM}	[m]	2.4	2.5	3.1		*12.7*	*12.0*	*3.4*					

Table 1. Test program with systematic parameter variation including Tests 1–27, and Tests 28–30 related to Kárahnjúkar project, all in prototype dimensions.

head H as elevation difference between the jet take-off level and the transmitter-level was kept constant at 92.5 m, all in prototype dimensions (*Fig. 2b*). Small discharges as compared to PMF were tested to keep the footprint on the riverbed, thereby avoiding an effect of the canyon flanks. Discharges are expressed with the critical flow depth $h_c = (q^2/g)^{1/3}$, where $q = Q/b$. In total, 27 tests were conducted with $1.1 \le b/Y \le 5.9$ and $0.2 \le h_c/Y \le 1.2$. The present results therefore by far exceed the test program of the original spillway investigation including a systematic parameter variation, as noted from the test program (*Table 1*, Tests 1–27). Test series were conducted by varying one parameter, e.g. Q, and keeping the other two parameters constant, e.g. b and Y. As a consequence, the isolated effect of each parameter on P_{da} resulted. Furthermore, selected tests of the Kárahnjúkar investigation (Tests 28–30) were considered with Q up to 950 m³/s, yet with isolated pressures affected by the opposite rock flank and a chute aerator, such that these were excluded for the data analysis.

4. Jet footprint

The grid for pressure measurements on the riverbed covered the entire canyon width, i.e. the entire jet footprint as the zone of notable jet-induced dynamic pressures. To define the footprint area, two criteria were applied: (1) $P_{da}/H \ge 0.1 h_c/Y$, and (2) $P_{da} \ge 2.0$ m in absolute terms for model measurement reasons. The pressure head of criterion (1) corresponds to half of the maximum value detected within the footprint, as shown below. Transmitters whose measured heads satisfied both criteria were considered located within the jet footprint. The two criteria resulted from an extensive data analysis; absolute offset values as a function of e.g. H resulted in poorly-defined footprint areas, especially for tests with small Q and large b and Y.

Figure 3 shows an example of three footprints, where b was varied, for otherwise constant parameters. The streamwise axis x corresponds to the chute centre line, with the transverse coordinate y perpendicular to x. Note that the footprint spreads with increasing b, is U-shaped and relevant pressures are concentrated laterally. The U-shaped footprint originates from a slightly smaller lateral chute velocity due to wall friction, with a reduced jet take-off velocity generating shorter lateral jet trajectories as compared to the chute centre flow. The relative thickness of a narrow jet is larger than of a wide, such that the footprint concentrates near the chute axis around $y = 0$. In contrast, the jet is thinner for a wide chute end, such that the footprint locally even disappears close to $y = 0$. In parallel, small chute flow depths imply higher energy losses, such that the jet take-off velocity slightly decreases, shifting the footprint towards the chute end.

The individual P_{da} of all transmitters located within the footprint were summed up to ΣP_{da} and divided by the transmitter number n located within the footprint. The data were then normalized with the jet impact head H and plotted versus h_c/Y. Consequently, the footprint area-averaged dynamic pressure head is

$$\frac{\sum P_{da}}{nH} = 0.15 \frac{h_c}{Y} \quad \text{for } 0 < h_c/Y < 1.2 \tag{5}$$

with a coefficient of determination of $R^2 = 0.95$ between the model data and Eq. (5). The lower limit was set to $h_c/Y = 0$, whereas the data only include $h_c/Y \ge 0.17$, because $P_{da}(h_c/Y \to 0) \to 0$. *Figure 4* compares the measured data with Eq. (5). Note that the footprint is located close to the opposite canyon flank for large discharges. Then, a distinction between footprint and wall effect was difficult, such that unfiltered data may include small wall effects in Eq. (5).

5. Effects of chute end width, discharge and plunge pool depth

5.1 Individual effect

The characteristic pressure heads P_{da} were derived for all grid points, of which the maximum (subscript M) P_{daM} within the footprint area was selected for further analysis to investigate the effects of b, Q, and Y. The long chute upstream of the take-off generates fully developed turbulent approach flow with uniform flow conditions for the tested discharges. The

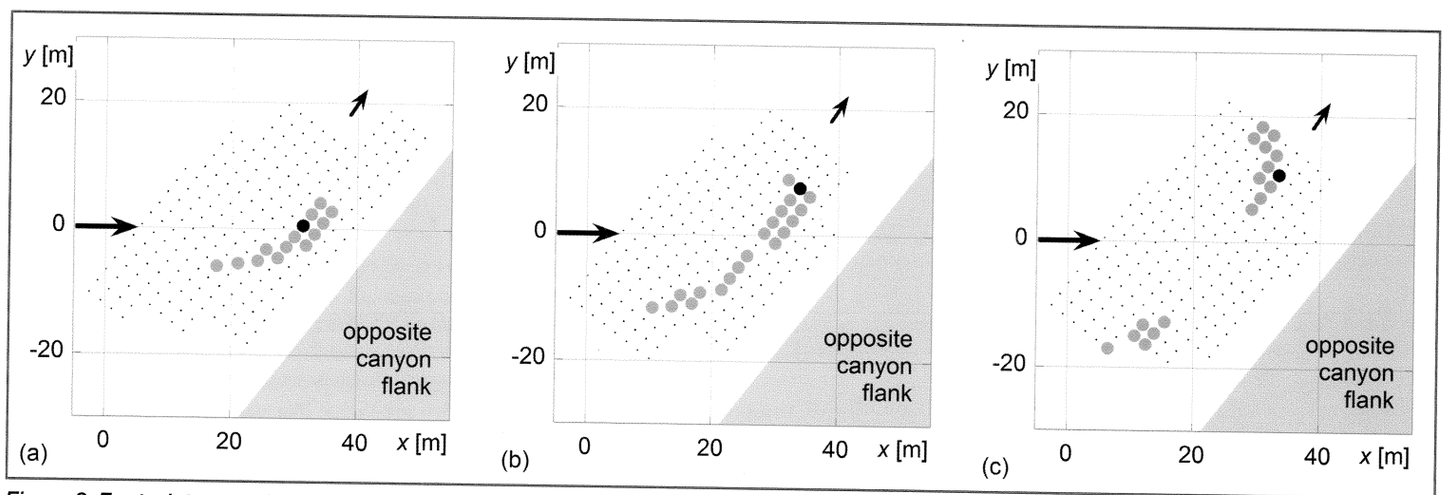

Figure 3. Footprint example of Tests (a) 3, (b) 12, and (c) 21, i.e. for increasing b, with (•) transmitter location, (•) footprint area, and (•) maximum P_{daM}.

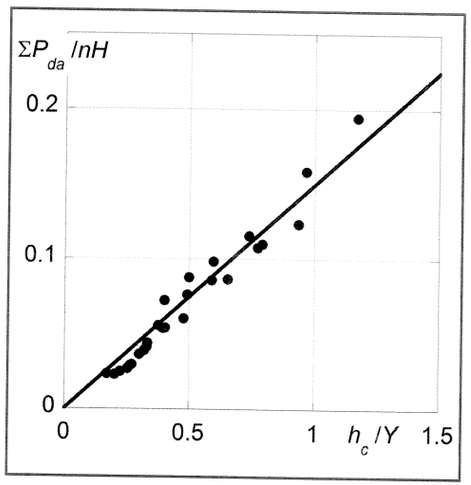

Figure 4. Footprint area-averaged dynamic pressure head $\Sigma P_{da}/nH[h_c/Y]$ with (–) Eq. (5).

measured average maximum P_{daM} of all tests was 21.3 m *(Table 1)*, corresponding to 23% of H. This is a relatively small value, pointing at pronounced jet disintegration. Almost immediately beyond take-off, the jet is fully-aerated below some 3 to 7% of H (Pfister and Hager 2009), and breaks up at 14 to 22% of H (Ervine et al. 1997), reducing pressures drastically in the plunge pool.

Figure 5 shows the un-normalized isolated effects of Q, Y, and b on P_{daM} in prototype dimensions. Within a series consisting of three tests, only the discussed parameter varies, while the others remain unchanged. Note from *Fig. 5a* that P_{daM} almost linearly increases with Q. However, this effect is relatively small, as P_{daM} only slightly increases with Q. More relevant is Y *(Fig. 5b)*, involving a strong decrease of P_{daM} for large Y, similar to Ervine et al. (1997). The effect of b on P_{daM} is shown in *Fig. 5c*, indicating reduced pressures as b increases. The maximum time-averaged dynamic pressure head P_{daM} measured within the jet footprint therefore increases with discharge, but decreases with chute end width, and with deep plunge pools. The jet impact head H further affects plunge pool pressures, yet this parameter was kept constant herein.

5.2 Normalized results

The dynamic plunge pool pressures were normalized as P_{daM}/H and P'_{dM}/H to include the jet impact head (Khatsuria 2005). The additionally investigated parameters affecting the plunge pool pressures were normalized as $h_c/Y = [(Q/b)^2/g]^{1/3}Y^{-1}$ thereby including Q, b and Y. The model data of P_{daM} collapse with a linear trend line as *(Fig. 6a)*.

$$\frac{P_{daM}}{H} = 0.20\frac{h_c}{Y} \quad \text{for } 0<h_c/Y<1.2 \tag{6}$$

with $R^2 = 0.93$ between the model data and Eq. (6). The latter may be expressed as $P_{daM} = 0.2HY^{-1}Q^{2/3}b^{-2/3}g^{-1/3}$ to assess the effect of the single variables, indicating that the jet impact head H and the plunge pool depth Y are significant, whereas the chute end width b and the discharge Q are less relevant. Dividing Eq. (5) by Eq. (6) results in $(\Sigma P_{da}/n)/P_{daM} = 0.75$. Accordingly, the area-averaged footprint pressure head is equivalent to some 75% of the local maximum P_{daM}, independent of b, Q and Y. The individual measured data include a ratio of 60 to 100%, with an average around 77%.

The same abscissa normalization as for P_{daM} was used for P'_{dM}, again resulting in a linear trend as

$$\frac{P'_{dM}}{H} = 0.23\frac{h_c}{Y} - 0.03 \quad \text{for } 0<h_c/Y<1.2 \tag{7}$$

Figure 6b compares the data and Eq. (7), with $R^2 = 0.89$. Note that $P'_{dM}/H = 0$ for $h_c/Y<0.13$. Accordingly, fluctuating pressures are absent if hc is sufficiently small, i.e. for a small q combined with large values Y corresponding to ‹deep› plunge pools, resulting in small P_{daM}, combined with $P'_{dM} = 0$. The jet momentum affects the plunge pool bottom, while the jet fluctuations are fully damped by the water cushion.

As explained, P_{daM} refers to the transmitter with the maximum measured average value of the entire footprint. To ensure its relevance, the next smaller maxima M2 and M3 were considered, with M1 representing the maximum P_{daM}, and M2 as well as M3 the next smaller values at a different transmitter. These are shown in *Fig. 7a*, which corresponds basically to *Fig. 6a* plus the further maxima. All values M1 to M3 almost collapse, such that recording errors may be excluded. In parallel, linear best fits were added to the figure, indicating a slight decay of the gradients for M1→M3. Accordingly, M2 and M3 are marginally lower than the absolute maximum M1. The same trend follows from *Fig. 7b*, showing the ratios of M2/M1 and M3/M1, respectively. In average, M2 is some 91% of M1, and M3 is roughly 87% of M1, including the few outliers. The latter represent tests with minimum Q and Y.

The pressure coefficients were again derived as a function of hc/Y. The dynamic coefficient collapses with a linear trend line as ($R^2 = 0.93$)

$$C_{da} = 0.15\frac{h_c}{Y} \quad \text{for } 0<h_c/Y<1.2 \tag{8}$$

The fluctuating coefficient was expressed as ($R^2 = 0.84$)

$$C'_d = 0.18\frac{h_c}{Y} - 0.03 \quad \text{for } 0<h_c/Y<1.2 \tag{9}$$

The data of both coefficients are shown in *Fig. 8* including Eqs. (8) and (9), indicating good agreement between measurements and predictions. Again, the fluctuating pressure coefficient is zero for $h_c/Y<0.13$, as the fluctuating pressure head was.

Dividing Eq. (8) by Eq. (6) results in $C_{da}/(P_{daM}/H) = 0.75$. Accordingly, the dynamic pressure coefficients are 75% of the relative dynamic pressure head, independent of b, Q and Y. From Eq. (2) then follows the jet net head $v_j^2/2g = 1.3H$. For the present tests, the gross jet energy head at impact on the plunge pool water surface is H plus the velocity head at take-off, which is between 0.3 and 0.5H. Accordingly, the difference of the gross jet head equivalent to 1.3 to 1.5H and the net jet head with 1.3H ranges between 0 and 0.2H, probably related to jet dissipation effects.

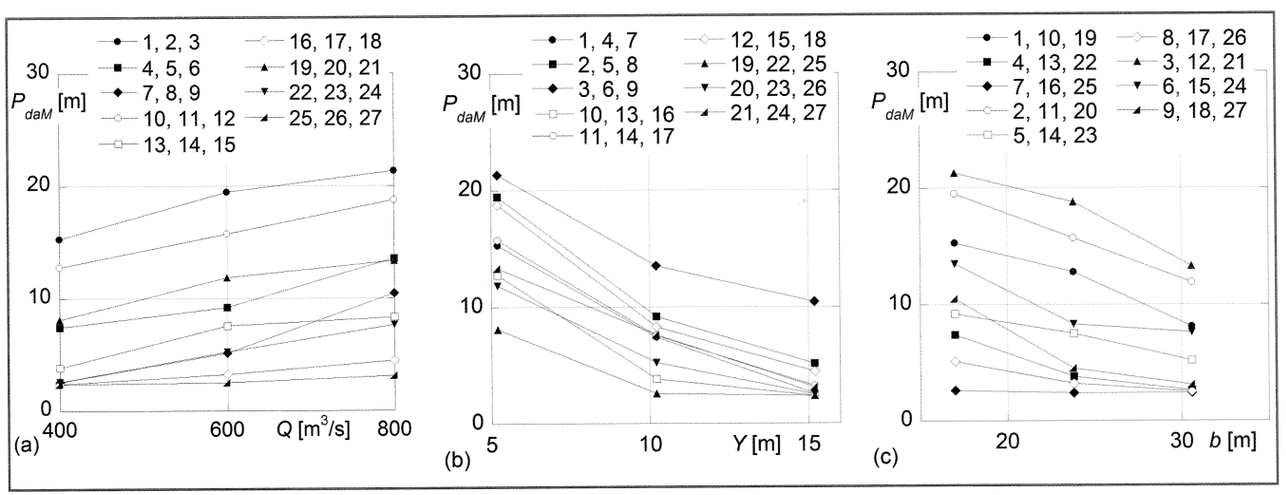

Figure 5. Individual effect of (a) Q, (b) Y, and (c) b on P_{daM}, Test number according to Table 1.

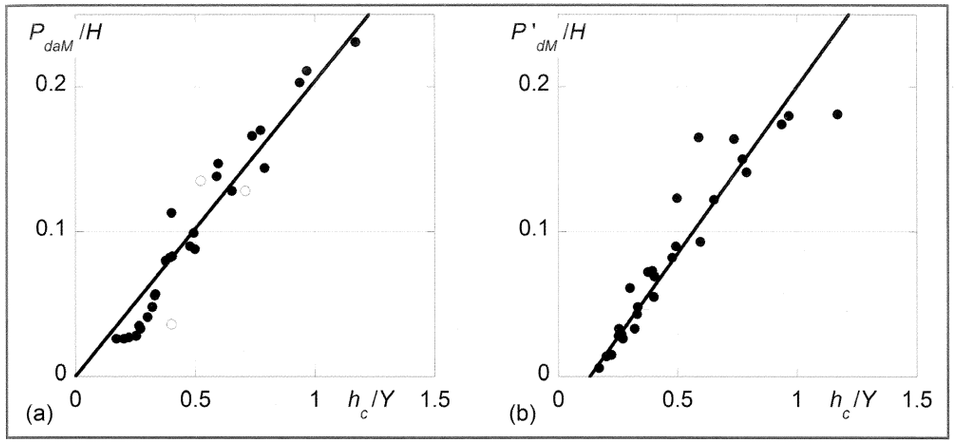

Figure 6. (a) $P_{daM}/H[h_c/Y]$ with (–) Eq. (6) and (○) Tests 28–30, and (b) $P'_{dM}/H[h_c/Y]$ with (–) Eq. (7).

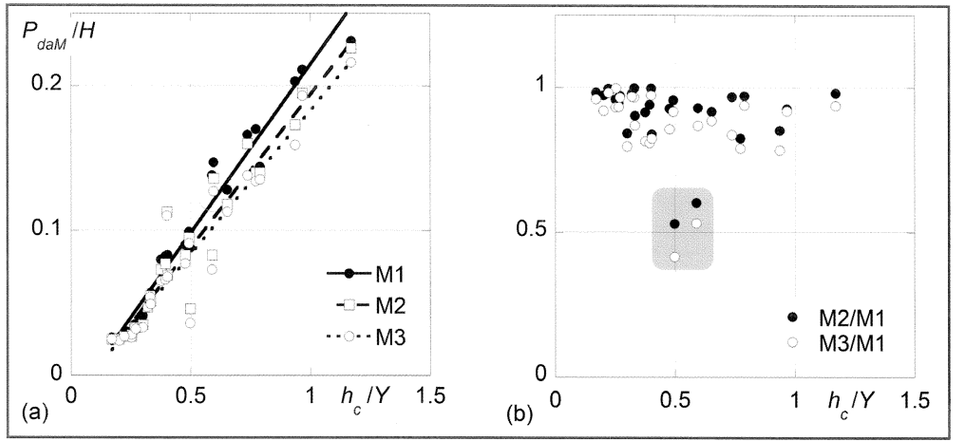

Figure 7. (a) Maxima M1 to M3 of $P_{daM}/H[h_c/Y]$ with trend lines and (b) ratios M2/M1 and M3/M1 relative to h_c/Y, outliers in grey.

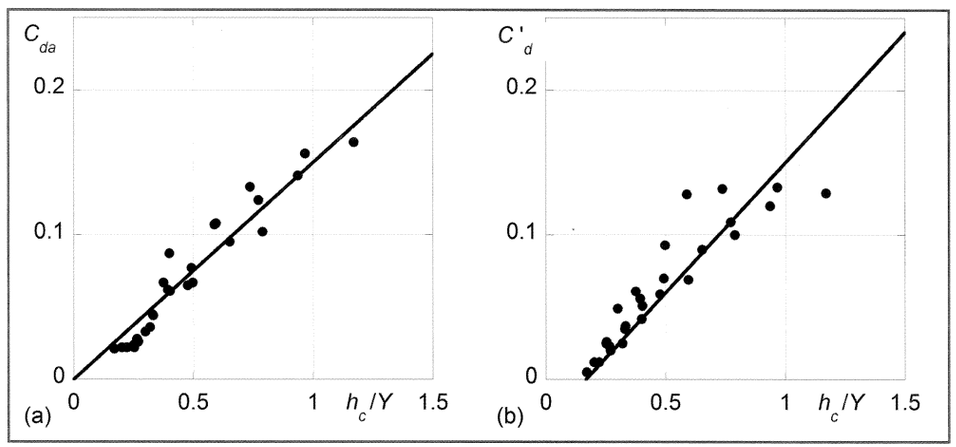

Figure 8. (a) $C_{da}[h_c/Y]$ with (–) Eq. (8), and (b) $C'_d[h_c/Y]$ with (–) Eq. (9).

6. Effect of baffles

Baffles or splitters mounted at the chute end generate considerable turbulence in the jet, enhancing its break-up and thereby generating low plunge pool pressures (Mason 1983). During the investigation of Kárahnjúkar Dam spillway, various baffle shapes and arrangements were model-tested. The final spillway design includes seven baffles with width to height dimensions of 0.5 × 0.5 m *(Fig. 9a)* and 3.8 m spacing between their individual axes, defined parallel to the chute centre line. To avoid cavitation damage, their side faces are inclined by 5V:3H and their edges rounded (Minor 1988). The baffles are mounted flush with the edge of chute end.

Equation (6) describes the dynamic maximum pressure head without baffles. The baffle (subscript *B*) effect follows the linear trend as ($R^2 = 0.91$)

$$\frac{P_{daBM}}{H} = 0.10\frac{h_c}{Y} \quad \text{for } 0<h_c/Y<1 \tag{10}$$

Dividing Eq. (10) by Eq. (6) results in the factor 0.5, i.e. the maximum time-averaged dynamic pressure head within the footprint area is halved by the baffles employed. The five considered baffle tests of *Fig. 9b* are not listed in *Table 1* but were derived from the Kárahnjúkar investigation, including 400 m³/s≤*Q*≤1350 m³/s, 2.7≤*b*/*Y*≤4.7 and 0.4≤h_c/Y≤0.9. No systematic parameter analysis was conducted here.

The design of Kárahnjúkar Dam spillway including the plunge pool was described by Pfister et al. (2008). The measured bottom pressures were drastically reduced as compared to the initial design, as indicated by the following example. For *Q* = 600 m³/s, the computed values for (1) the initial design were P_{daM} = 17.5 m provided *b* = 17.0 m, *Y* = 5.2 m without baffles, and (2) for the final design amounted to P_{daM} = 4.8 m if *b* = 30.6 m, *Y* = 6.5 m with baffles. The measured values decreased from P_{daM} = 19.5 to 3.8 m, i.e. reduced to roughly 1/5. *Figure 10* shows the prototype jet resulting for the widened chute end equipped with baffles, pointing at strong jet disintegration.

7. Conclusions

Measures to reduce dynamic plunge pool pressures generated by a free jet are discussed, including jet expansion by terminal chute widening, provision of baffles at the chute end, and increase of the plunge pool depth. The effect of these parameters was investigated using a hydraulic model with a systematic parameter variation. The dynamic and fluctuating pressure heads on the plunge pool bottom were thereby considered as reference values. For the present case study, the jet impact head *H* and the plunge pool depth *Y* are relevant, whereas the chute end width *b* and the discharge *Q* are of lower significance. Equations were derived to predict the determining pressures within the limitations of the model investigation. It was further demonstrated that baffles effectively reduce dynamic pressure heads. The model limitations relate to the jet fall height, the discharge spectrum and the plunge

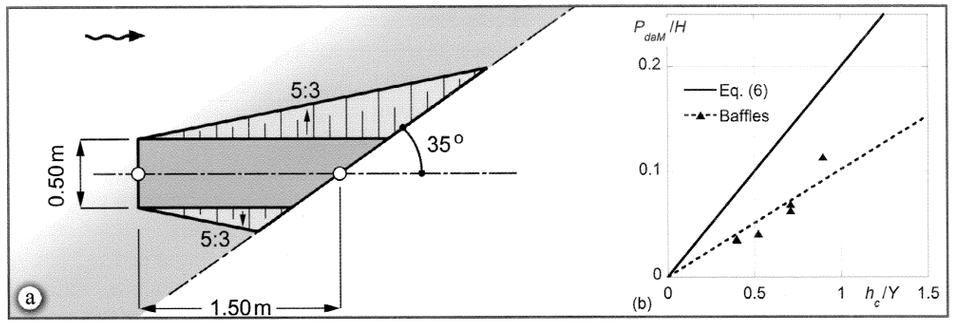

Figure 9. (a) Plan view of baffles, and (b) comparison of (–) Eq. (6) without, and (---) Eq. (10) with baffles.

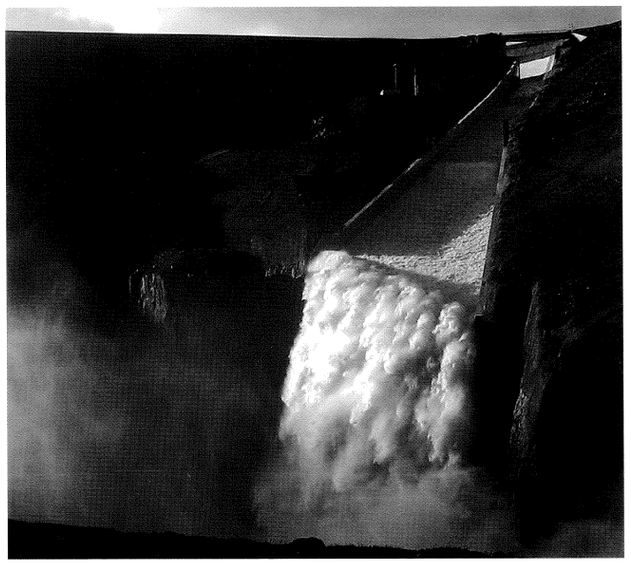

Figure 10. Prototype spillway flow and jet pattern for approximately 200 m³/s (courtesy Landsvirkjun).

pool arrangement, resulting from the Kárahnjúkar Dam spillway investigation, for which the model was initially erected.

8. Acknowledgments

The authors thank Landsvirkjun for excellent collaboration and provision of the project data set. Measurements not directly related to the Kárahnjúkar Dam project were conducted by Melanie Wyss. The support of Adriano Lais and Prof. Dr. Hans-Erwin Minor, both then at VAW, is acknowledged.

References

Annandale, G.W. (2005). Scour technology. McGraw-Hill, New York.

Bollaert, E.F.R., and *Schleiss, A.J.* (2003a). Scour of rock due to the impact of plunging high velocity jets, Part I: A state-of-the-art review. Journal of Hydraulic Research 41(5), 451–464.

Bollaert, E.F.R., and *Schleiss, A.J.* (2003b). Scour of rock due to the impact of plunging high velocity jets, Part II: Experimental results of dynamic pressures at pool bottoms and in one- and two-dimensional closed end rock joints. Journal of Hydraulic Research 41(5), 465–480.

Bollaert, E.F.R., and *Schleiss, A.J.* (2005). Physically-based model for evaluation of rock scour due to high velocity jet impact. Journal of Hydraulic Engineering 131(3), 153–165.

Canepa, S., and *Hager, W.H.* (2003). Effect of jet air content on plunge pool scour. Journal of Hydraulic Engineering 129(5), 358–365.

Ervine, D.A., and *Falvey, H.T.* (1987). Behavior of turbulent water jets in the atmosphere and in plunge pools. Proc. Instn Civ. Engrs 83(2), 295–314, Paper 9136.

Ervine, D.A, Falvey, H.T, and *Withers, W.* (1997). Pressure fluctuations on plunge pool floors. Journal of Hydraulic Research 35(2), 257–279.

Fiorotto, V. and *Rinaldo, A.* (1992). Turbulent pressure fluctuations under hydraulic jumps. Journal of Hydraulic Research 30(4), 499–520.

Khatsuria, R.M. (2005). Hydraulics of spillways and energy dissipators. Dekker, New York.

Li, A., and *Liu, P.* (2010). Mechanism of rock-bed scour due to impinging jet. Journal of Hydraulic Research 48(1), 14–22.

Lopardo, R.A. (1988). Stilling basin pressure fluctuation. Proc. Intl. Symposium on Model-Prototype Correlation of Hydraulic Structures, Colorado Springs, USA, 56–73.

Manso, P.A., Bollaert, E.F.R., and *Schleiss, A.J.* (2007). Impact pressures of turbulent high-velocity jets plunging in pools with flat bottom. Experiments in Fluids 42(1), 49–60.

Mason, P.J. (1983). Energy dissipating crest splitters for concrete dams. International Water Power & Dam Construction 35(11), 37–40.

Minor, H.-E. (1988). Konstruktive Details zur Vermeidung von Kavitationsschäden. Mitteilung 99, D. Vischer ed., Laboratory of Hydraulics, Hydrology and Glaciology, ETH, Zurich, 367–378 [in German].

Pagliara S., Hager, W.H., and *Minor, H.-E.* (2006). Hydraulics of plunge pool scour. Journal of Hydraulic Engineering 132(5), 450–461.

Pfister, M., Berchtold, T., and *Lais, A.* (2008). Kárahnjúkar dam spillway: Optimization by hydraulic model tests. 3rd IAHR International Symposium in Hydraulic Structures, Hohai University, Nanjing (Cn), VI, 2106–2111.

Pfister, M., and *Hager, W.H.* (2009). Deflector-generated jets. Journal of Hydraulic Research 47(4), 466–475.

Puertas, J., and *Dolz, J.* (2005). Plunge pool pressures due to a falling rectangular jet. Journal of Hydraulic Engineering 131(5), 404–407.

Schmocker, L., Pfister, M., Hager, W.H., and *Minor, H.-E.* (2008). Aeration characteristics of ski jump jets. Journal of Hydraulic Engineering 134(1), 90–97.

Tómasson, G.G., Garðarsson, S.M., Petry, B., and *Stefánsson, B.* (2006). Design challenges and solutions for the Kárahnjúkar spillway. Hydropower & Dams 13(5), 84–88.

VAW (2006). Kárahnjúkar HEP Iceland; Physical model investigation on the Kárahnjúkar dam spillway. VAW Report 4203, ETH: Zurich [unpublished]

Vischer, D.L. and *Hager, W.H.* (1998). Dam hydraulics. John Wiley & Sons, Chichester, UK.

Authors:

Thomas Berchtold
Laboratory of Hydraulics, Hydrology and Glaciology (VAW), ETH Zurich, CH-8092 Zurich, Switzerland
berchtold@vaw.baug.ethz.ch

Michael Pfister
Laboratory of Hydraulic Constructions (LCH), Ecole Polytechnique Fédérale de Lausanne (EPFL), EPFL-ENAC-LCH, Station 18, CH-1015 Lausanne, Switzerland. Formerly: VAW, ETH Zurich.
michael.pfister@epfl.ch

Cover: Emosson-Dam
Photo: Claude Darbellay

www.swissdams.ch

ISBN 978-3-85545-158-6

Editing Committee:
Working Group «Public Relations» of the Swiss Committee on Dams

Layout:
Manuel Minder

Printed by:
buag, Grafisches Unternehmen AG
Täfernstrasse 14, CH-5405 Baden-Dättwil

Print run:
2000 Ex. (May 2011)